CONF-961203--39 SAND97-0177C

# NATURE OF THE GREEN LUMINESCENT CENTER IN ZINC OXIDE

K. VANHEUSDEN*, W. L. WARREN*, C. H. SEAGER*, D. R. TALLANT*
J. CARUSO**, M. J. HAMPDEN-SMITH**, T. T. KODAS**
*Sandia National Laboratories, Albuquerque, New Mexico 87185-1345
**Nanochem Research Inc., 11102 San Rafael NE, Albuquerque, New Mexico 87122



## ABSTRACT

We apply a number of complementary characterization techniques including electron paramagnetic resonance, optical absorption, and photoluminescence spectroscopies to characterize a wide range of different ZnO phosphor powders. We generally observe a good correlation between the 510-nm green emission intensity and the density of paramagnetic isolated oxygen vacancies. In addition, both quantities are found to peak at a free-carrier concentration $n_e$, of about $1.4 \times 10^{18}$ cm$^{-3}$. We also find that the green emission intensity can be strongly influenced by free-carrier depletion at the particle surface, especially for small particles and/or low doping. Our data suggest that the green PL in ZnO phosphors is due to the recombination of electrons in singly occupied oxygen vacancies with photoexcited holes in the valence band.

## INTRODUCTION

In order to guide the design of new phosphor materials, or improve the efficiency of established phosphors, the physical mechanisms behind their luminescence must be understood. ZnO material for example, a high-efficiency low-voltage phosphor, has recently regained much interest because of its potential use in new low-voltage luminescence applications, such as the field emissive display technology. It is now quite commonly accepted that the green luminescence in ZnO arises from a radiative recombination involving an intrinsic defect center [1-5]. Surprisingly however, the exact nature of the recombination center and mechanism responsible for the green luminescence in ZnO are still a matter of controversy.

In the present work, we use a number of complementary characterization techniques such as electron paramagnetic resonance (EPR), optical absorption, and photoluminescence (PL) spectroscopies to obtain a better understanding of the physics underlying the luminescent process in ZnO phosphor powders. Samples studied include different commercially available ZnO powders and high purity ZnO powders fabricated using spray pyrolysis [6]. Our data show a strong correlation between the green luminescence, the paramagnetic oxygen-vacancy concentration, and the free-carrier concentration. Many features of our data are explained by taking into account the effects of the Fermi level position in the ZnO gap and free-carrier depletion at the particle surface. We conclude that the defect center responsible for green luminescence is the isolated singly-ionized oxygen vacancy center.

## EXPERIMENTAL TECHNIQUES



### Sample preparation

Two different commercial phosphor powders: ZnO (powder A) and ZnO:Zn (powder B) were obtained from Fisher and Sylvania, respectively. A third type of ZnO powder (powder C) was synthesized using a bench scale spray pyrolysis reactor, utilized by *Nanochem Research, Inc.* All aerosols were generated by an ultrasonic transducer from an aqueous zinc nitrate (99.999 %) solution (10 wt. % Zn). The ultrasonically generated aerosol was passed through the reactor with either air, nitrogen or forming gas [$N_2$:$H_2$; 93:7 (by volume, 99.999% pure)] at various furnace temperatures (700-900 °C).

Where indicated, additional post-synthesis reduction and oxidation treatments were performed in a flow of forming gas [$N_2$:$H_2$; 95:5 (by volume, 99.999% pure)] or pure $O_2$

## DISCLAIMER

(99.999% pure), respectively, through a single-wall quartz tube, with a flow rate of ≈ 1 *l* /min. The tube was inserted into a resistance-heated tube furnace, maintained at a constant (±1 °C) temperature. The powders were placed on a quartz boat and inserted into the preheated furnace. Following the anneals, the boat was pulled out of the tube furnace and quenched in air to room temperature. The reduction treatments in forming gas (FG) ambient were observed to cause significant release of Zn vapor. The amount of Zn released increased strongly with temperature. The release of Zn was not observed when annealing the powders in pure $N_2$, a less reducing ambient. Powder particle sizes were determined from scanning-electron-microscopy imaging, ranging from 50-400 nm for powder A, 500-1500 nm for powder B, and 400-1000 nm for powder C.

Analysis techniques

To obtain accurate optical absorption data for powders normal transmission techniques are not appropriate because of strong scattering of the transmitted beam. To minimize these scattering effects a calorimetric technique was employed known as photothermal deflection spectroscopy (PDS). This technique monitors the optical energy absorbed in the sample by detecting the temperature rise in an adjacent liquid medium (Fluorinert) with a laser deflection method [7,8]. The absorption coefficient $\alpha(E)$ obtained by this technique has been calibrated by using powder obtained from single crystal ZnO. The free-carrier concentration ($n_e$) can be calculated from the free-carrier absorption [9]. While the absolute accuracy of deducing the free-carrier concentration is estimated at ±50%, the error in deducing changes in $n_e$ from sample to sample is considerably smaller.

Two different excitation energies were used to obtain photoluminescence (PL) emission spectra: continuous-wave, near UV excitation at 370 nm from a Xe lamp as filtered through a double monochromator; and pulsed far-UV laser excitation at 232 nm from a Nd:YLF laser/ optical parametric oscillator source. Excitation intensities were in the mW/cm$^2$ range. Fluorescence spectra were recorded using a charge-coupled detector linked to a 0.6-m spectrograph.

EPR measurements were performed using an *X*-band (≈ 9.430 GHz) Bruker ESP-300E spectrometer between 4.3 and 294 K. Cylindrical quartz tube containers were used to insert the powders into the microwave cavity. Photo-EPR measurements were performed as well by using thin powder films between two quartz platelets and an optical access microwave cavity.

## EXPERIMENTAL RESULTS

In all samples two predominant paramagnetic defects were observed. The EPR signals are spectrally close to each other: one broad resonance with g = 1.9596 and one narrower line with g = 1.9564. Both signals are observable from 4.3 K to 294 K and are attributed to the singly ionized oxygen vacancy ($V_O^\bullet$) defect. Since both signals are spectroscopically so close to each other, the broader g = 1.9596 signal has been attributed to some distortion of the original narrow signal [1], probably caused by a nearby interstitial oxygen (Frenkel pair) [10]. We will refer to the latter defect as the $V_O^\bullet$-complex, as opposed to the narrow signal which is simply an isolated $V_O^\bullet$. Only the isolated-$V_O^\bullet$ signal was observed to be largely affected by the oxidation and reduction anneals. Also, in certain samples the isolated-$V_O^\bullet$ signal grows strongly upon illumination while the $V_O^\bullet$-complex signal shows no photosensitivity. The rest of this work will focus on the isolated-$V_O^\bullet$, which wil be simple refered to as $V_O^\bullet$. As explained above, $n_e$ was derived from the optical absorption spectrum. The 510-nm green fluorescence intensities were obtained by integrating the PL emission spectrum (using 370 nm excitation). In addition to the green PL, UV fluorescence peaking near 390 nm, could also be observed using the 232-nm excitation source. No direct correlation could be established between the intensity of the green and the UV PL bands. This suggests that they originate from different sites in the ZnO phosphor.

Figure 1 shows the dark concentration (no illumination) of paramagnetic $V_O^\bullet$, the free-carrier electron concentration ($n_e$), and the intensity of the green emission peak for the type-A ZnO powder as a function of FG anneal temperature. These data show a correlation between the

intensity of the green emission, the dark density of $V_O^{\bullet}$, and $n_e$. Notice the large difference in absolute scale between the $V_O^{\bullet}$ density and $n_e$. This strongly suggests that the $V_O^{\bullet}$ center is not the primary donor dopant in ZnO. The $V_O^{\bullet}$ EPR signal was observed to be photosensitive for photon energies as low as 2.3 eV, as has been observed previously [11,12]. After extended broad-band illumination, the $V_O^{\bullet}$ density was observed to saturate at $\approx 2.5 \times 10^{15}$ cm$^{-3}$ in all the type-A samples studied.

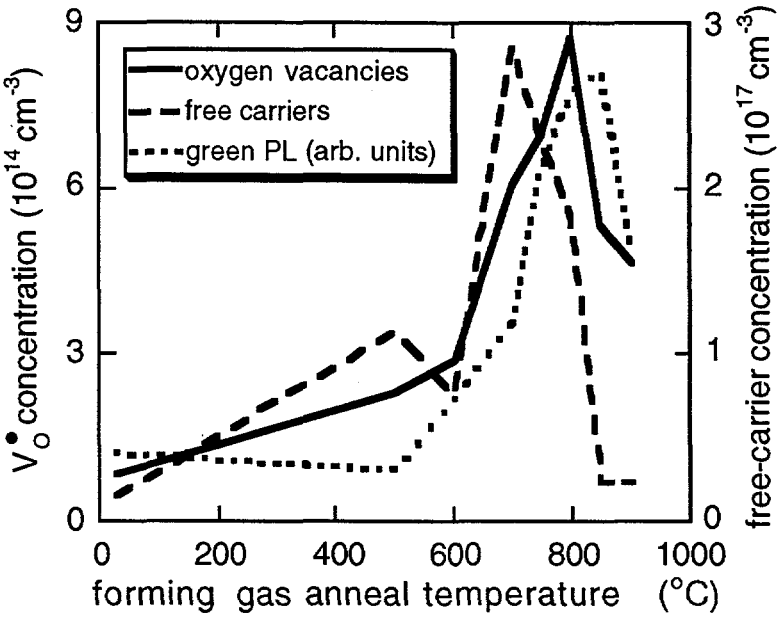


FIG. 1. Intensity of the green emission peak, free-carrier (electron), and singly-ionized oxygen vacancies ($V_O^{\bullet}$) concentration as a function of reduction anneal temperature for ZnO powder A (Fisher). Anneals were performed in a flow of forming gas [$N_2$:$H_2$; 95:5 (by volume)] for 20 min at a flow rate of $\approx 1$ *l*/min. All data were recorded at 294 K.

The initial (untreated) type-B ZnO:Zn powder starts with much more intense green PL and higher $n_e$ than the type-A ZnO powder (approximately 50 times greater), so the effects of oxidation treatments was investigated on this phosphor. Figure 2 shows the $V_O^{\bullet}$ (dark) density and the $n_e$ values, together with the intensity of the green emission peak for the ZnO:Zn powder (type B) as a function of isochronal oxidation temperature. Again, a reasonable correlation is observed between the density of $V_O^{\bullet}$, green PL, and $n_e$, i.e., the three parameters drop roughly one order of magnitude between 700 and 1050 °C. As for the type-A ZnO, 232-nm excitation results in a UV band in addition to the green band, again both showed no correlation. However, the UV band in the type-B samples is typically one order of magnitude smaller than in the type-A powders. Note that this is opposite to the trend observed for the green band intensities; the green PL is roughly 50 times greater in the type-B phosphors. It is also important to note that the $V_O^{\bullet}$ signal did not display any significant photosensitivity in the type-B powders (as-prepared or after oxidation). This suggests that essentially all of the oxygen vacancies are in their singly-ionized paramagnetic $V_O^{\bullet}$ state.

Finally, type-C spray-pyrolysis ZnO powders were analysed. By varying the carrier-gas and temperature during spray pyrolysis and post-processing reduction annealing, a wide range of $n_e$ values were obtained: $n_e$ was found to be enhanced by spray pyrolysis performed using forming gas as the carrier gas and/or by post synthesis reduction anneals in forming gas. Figure 3 shows the concentration variations of the paramagnetic $V_O^{\bullet}$ defect and the 510-nm green-emission efficiency for 370-nm excitation as a function of the free-carrier concentration in the various ZnO samples. Both the $V_O^{\bullet}$ defect density and the green emission intensity peak at $n_e \approx 1.4 \times 10^{18}$ cm$^{-3}$, decreasing at lower and higher free-carrier concentrations. An analogous

behavior was observed for the green luminescence at 230-nm excitation. Finally, the isolated-$V_O^{\bullet}$ signal in the type-C powders was enhanced upon illumination., but this effect strongly decreased with increasing $n_e$.

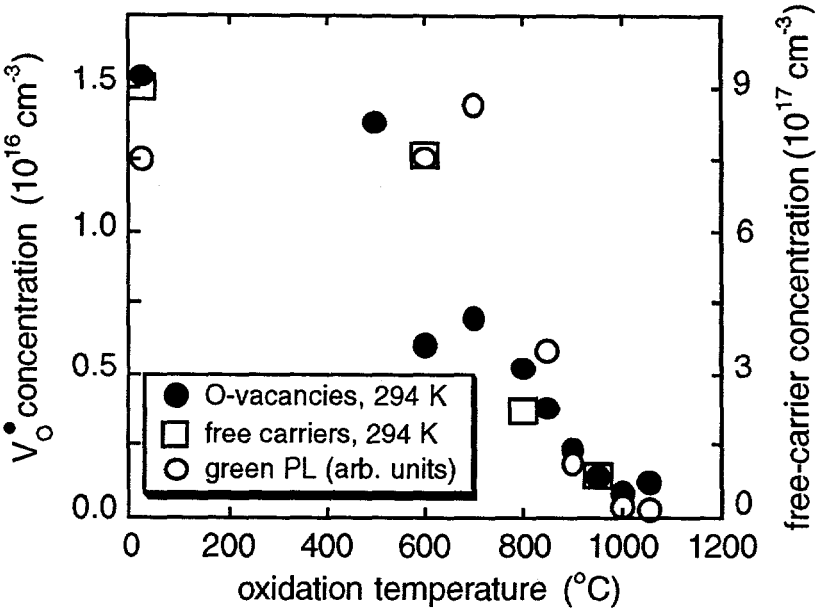


FIG. 2. Intensity of the green emission peak, free-carrier (electron), and singly-ionized oxygen vacancies ($V_O^{\bullet}$) concentration vs. oxidation anneal temperature for type-B ZnO (Sylvania). Anneals were performed in a flow of $O_2$ for 1 h at a flow rate of $\approx$ 1 *l* /min. All data were recorded at 294 K.

## DISCUSSION

One general conclusion from Figs 1, 2, and 3 is the close correlation between the paramagnetic isolated-$V_O^{\bullet}$ centers and the green PL intensity for all the 3 different samples studied. It is thus suggested that the obvious mechanism responsible for the green emission is recombination of $V_O^{\bullet}$ electrons with photoexcited holes in the valence band

### Oxygen vacancy centers and free-carrier concentrations

Oxygen vacancies in ZnO can occur in three different charge states: the $V_O^0$ state which has captured two electrons and is neutral relative to the lattice, the singly ionized $V_O^{\bullet}$ state, and the $V_O^{\bullet\bullet}$ state which did not trap any electrons and is doubly positively charged with respect to the lattice. Only the $V_O^{\bullet}$ state is paramagnetic, and consequently observable by EPR. Because the $V_O^0$ state is assumed to be a very shallow donor [11], it is expected that the oxygen vacancies will predominantly be in their paramagnetic $V_O^{\bullet}$ state under flat band conditions. As can be seen from Figs. 1, 2, and 3, there exists a good correlation between $n_e$ and the isolated-$V_O^{\bullet}$ concentration (without illumination) for $n_e$ values below $1.4 \times 10^{18}$ cm$^{-3}$. Although the oxygen vacancy is an intrinsic donor [13] in ZnO, the coexistence of another donor, probably excess Zn [12] at interstitial sites [14], with a much higher density must be inferred to explain the large differences between the $V_O^{\bullet}$ and the free-carrier densities in all of the powders studied here.

From the dependence of the green PL efficiency on the free-carrier (conduction-electron) concentration as shown in Fig. 3, it seems that there exists an optimum $n_e$ value for green PL efficiency which is $\approx 1.4 \times 10^{18}$ cm$^{-3}$. The decline in green PL efficiency at higher $n_e$ values is tentatively attributed to a Fermi-level effect. The effective density of states in the ZnO

conduction band can be calculated to be about $5.7 \times 10^{18}$ cm$^{-3}$. Since the conduction-electron concentrations in the type-C powders reach or even exceed this value, the Fermi-level will be located very close to the conduction band. As a result, the isolated singly-ionized $V_O^{\bullet}$ center may well change its ionization state to the neutral, diamagnetic (not observable by EPR) $V_O^0$ state in the powders with the highest free-carrier concentration, thus decreasing the density of the species responsible for the green PL. The latter assumption is in agreement with the steep drop in the isolated-$V_O^{\bullet}$ signal intensity with increasing $n_e$ as shown in Fig 3. Finally, the decline in green PL efficiency for $n_e$ values above $1.4 \times 10^{18}$ cm$^{-3}$ suggests that the donor site itself (excess or interstitial Zn related) is not the active green luminescence center, as has been suggested in the past [13].

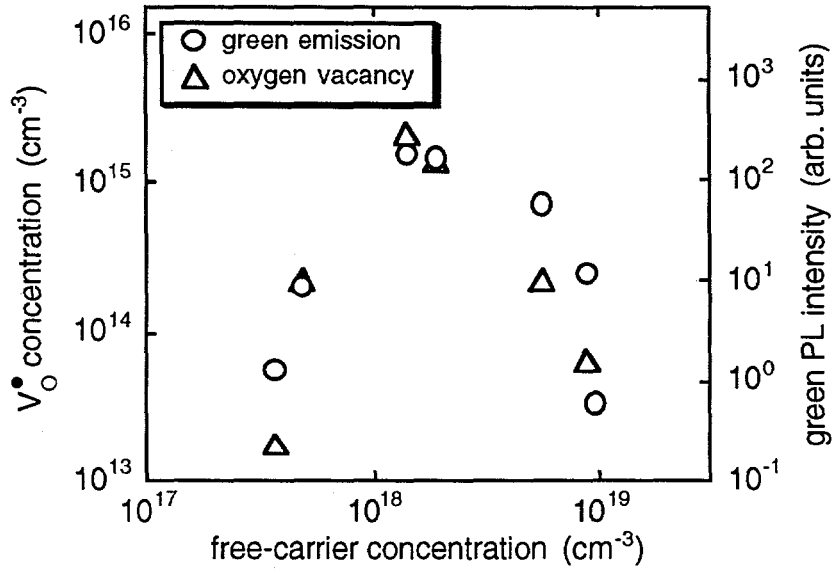


FIG. 3. Concentration of $V_O^{\bullet}$ defects and 510-nm green-emission efficiency as a function of the free-carrier concentration in type-C ZnO samples. The free-carrier concentration was obtained experimentally from the optical absorption spectrum.

Free-carrier depletion at particle surfaces

Band bending at ZnO powder particle surfaces should be considered [10,15] to explain correlations between $n_e$ and the ionization state of the oxygen vacancy and the resulting variations in PL intensity. Band bending will create an electron depletion region of width $W$ at the particle surfaces:

$$W = \sqrt{\frac{2\,\varepsilon_{ZnO}\,V_{bi}}{e\,N_D}}$$

where $V_{bi}$ is the potential at the boundary, $e$ is the electronic charge, $N_D$ is the donor density, and $\varepsilon_{ZnO}$ is the static dielectric constant of ZnO. Assuming that the depletion layer charge density ($N_D$) is roughly equal to the measured free-carrier concentration, and $V_{bi}$ is of the order of 1 V, the depletion layer width can be calculated to be roughly 100 nm for type-A and 30 nm for type-B powders (unannealed). Due to the difference in particle size, the depletion region will cover a significant fraction of the particles in the type-A ZnO powder (200-nm average particle size), whereas, for the larger-grained type-B ZnO powders (1-μm average particle size) with a higher free-carrier density, it only represents a few percent of the total volume. In the fraction of this region where the Fermi level passes below the $V_O^{\bullet}/V_O^{\bullet\bullet}$ energy level, all oxygen vacancies will be in the diamagnetic $V_O^{\bullet\bullet}$ state. Under sufficiently strong illumination, band bending can be

reduced as minority carriers are attracted to the surface and become trapped; this converts the $V_O^{\bullet\bullet}$ centers to the paramagnetic $V_O^{\bullet}$ state. The fact that the $V_O^{\bullet}$ signal is not photosensitive in the type-B powders, but highly photosensitive in the much smaller-grained type-A powders, supports the notion that surface band bending controls the photosensitivity of the $V_O^{\bullet}$ EPR signal. The particle size for the type-C powders is intermediate between type-A and type-B, and their depleted fraction depends on their free-carrier concentration. The width of the depletion region, and hence, the fraction of oxygen vacancies that is diamagnetic ($V_O^{\bullet\bullet}$) or PL-inactive, is inversely proportional to the square root of the free-carrier concentration in the particles. This explains why the green PL is found to increase with increasing $n_e$, for $n_e$ values below $1.4 \times 10^{18}$ cm$^{-3}$.

## SUMMARY AND CONCLUSIONS

Our data provide new information about the PL mechanisms responsible for green emission in ZnO. We observe a good correlation between the green emission intensity and the singly-ionized isolated oxygen vacancy density in a wide range of different ZnO powders. Based on these observations, we suggest that the green PL in ZnO phosphors is due to the recombination of electrons in singly occupied oxygen vacancies ($V_O^{\bullet}$) with photoexcited holes in the valence band. Both the green PL efficiency and the isolated vacancy density are observed to peak as a function of free-carrier concentration at a concentration of about $1.4 \times 10^{18}$ cm$^{-3}$. It is argued that at free-carrier densities below $1.4 \times 10^{18}$ cm$^{-3}$, free-carrier depletion at the particle surface plays a major role in the correlation between the free-carrier concentration, the density of singly-ionized isolated oxygen vacancies, and the green emission intensity. The decline of the green PL and paramagnetic isolated oxygen vacancy density at higher free-carrier densities is tentatively attributed to a change in the charge state of the luminescence center: $V_O^{\bullet} \rightarrow V_O^{0}$, as the ZnO becomes degenerate due to the high free-carrier density.

## ACKNOWLEDGMENT

This work performed at SNL was supported by the US Department of Energy under contract DE-AC04-94AL85000. Sandia is a multiprogram laboratory operated by Sandia Corporation, a Lockheed Martin Company, for the US DOE.

## REFERENCES

[1] P. H. Kasai, Phys. Rev. **130**, 989 (1963).
[2] N. Riehl and H. Ortman, Z. Elektrochem. **60**, 149 (1956).
[3] F. A. Kröger and H. J. Vink, J. Chem. Phys. **22**, 250 (1954).
[4] L. Ozawa, *Cathodoluminescence Theory and Applications,* (VCH Publishers, New York, NY, 1990), p. 255.
[5] K. Vanheusden, C. H. Seager, W. L. Warren, D. R. Tallant, and J. A. Voigt, Appl. Phys. Lett. **68**, 403 (1996).
[6] Y. Senzaki, J. Caruso, M. J. Hampden-Smith, T. T. Kodas, and L-M Wang, J. Am. Ceram. Soc. **78**, 2973 (1995); C. Roger, T. Corbitt, C. Xu, D. Zeng, Q. Powell, C. D. Chandler, M. Nyman, M. J. Hampden-Smith, and T. T. Kodas, Nanostructured Mater. **4**, 529 (1994); A. Gurav, T. Kodas, T. Pluym, Y. Xiong, Aerosol Sci. and Technol. **19**, 411, (1993).
[7] W. B. Jackson, N. M. Amer, A. C. Boccara, and D. Fournier, Appl. Opt. **20**, 1333 (1981).
[8] C. H. Seager and C. E. Land, Appl. Phys. Lett. **45**, 395 (1984).
[9] D. G. Thomas, J. Phys. Chem. Solids **9**, 31 (1958).
[10] K. Hoffmann and D. Hahn, Phys. Status Solidi A **24**, 637 (1974).
[11] A. Pöppl and G. Völkel, Phys. Status Solidi A **125**, 571 (1991).
[12] G. D. Mahan, J. Appl. Phys. **54**, 3825 (1983).
[13] M. Liu, A. H. Kitai, and P. Mascher, J. Luminescence **54**, 35 (1992).
[14] G. Heiland et al., Solid State Phys. **8**, 193 (1959).
[15] K. Vanheusden, W. L. Warren, J. A. Voigt, C. H. Seager, and D. R. Tallant, Appl. Phys. Lett. **67**, 1280 (1995).